1. Description of functionalised graphene

The C-C bond distances around the vacancy are given in Table S.1.All carbon atoms in graphene containing a mono-vacancy lie in one plane. The carbon–carbon distance around the vacancy for the coordinatively unsaturated carbon atoms is shortened by 0.04 Å to 1.38 Å compared to the C-C bond in pristine graphene of 1.42 Å (see Table S1) consistent with previous calculations.[S1] This is indicative of reduced resonance in the structure around C1, C5 and C9.

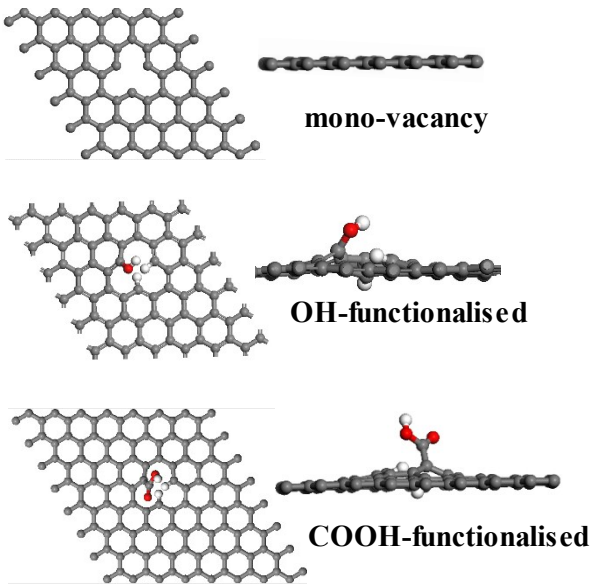

Figure S1. Optimised structures of mono-vacancy graphene, OH-functionalised graphene and COOH-functionalised graphene. *Grey*: carbon, *Red*: oxygen and *White*: hydrogen.

The OH-functionalised graphene contains besides the hydroxyl group at the vacancy also H-atoms. Different initial configurations of the OH-group at C1 and hydrogen at C5 and C9 in the vacancy were probed, viz. both hydrogen atoms and the hydroxyl group on the same side of the graphene sheet, and one or both hydrogen atoms separated from the hydroxyl group by the dividing plane given by the graphene sheet. All three unique starting configurations converged to the same final structure (shown in Fig. S1). The hydrogen atoms at C5 and at C9 are separated from the hydroxyl group by the dividing plane generated by the graphene sheet. The hydroxyl group is lifted out of the graphene plane. The distance between C1 and oxygen in the hydroxyl group is with 1.36 Å, similar to the calculated $d_{C\text{-}O}$ = 1.37 Å in phenol.[S2] The O-H distance is 0.98 Å and is the same as the calculated O-H distance in phenol.[38] C1 and the attached O-H bond make an angle of 109.1° (similar to calculated $\angle_{C-OH}$= 109.3° in phenol). [S2] The C-H bonds at C5 and C9 are almost parallel to the graphene sheet. The C-H bond at C9 makes an angle of 20.1° with the plane through graphene, resulting in an almost parallel orientation of the C-H bond to the graphene plane. The optimised position for carbon atom C5 is almost an inverted image of the position for C9.

Different initial configurations of COOH-functionalised graphene for the carboxyl group and the H atoms were investigated akin to OH-functionalised graphene. The optimised structure of COOH-functionalised graphene is similar to that for OH-functionalised graphene and shows a distortion of the structure around the vacancy (see Figure S1). The carboxyl group is tilted towards the vacancy. The carboxyl group has $d_{C=O}$ = 1.23 Å, $d_{C\text{-}O(H)}$ = 1.38 Å, $d_{O\text{-}H}$ = 0.98 Å, $d_{C\text{-}C(OOH)}$ = 1.47 Å and $\angle_{O=C-OH}$ = 120.8°. For comparison, reported DFT PW91 calculated bond lengths of benzoic acid are $d_{C=O}$ = 1.213 Å, $d_{C\text{-}O(H)}$ = 1.351 Å, $d_{O\text{-}H}$ = 0.974 Å, $d_{C\text{-}C(OOH)}$ = 1.482 Å and $\angle_{O=C-OH}$ = 119.1°.[S3] The C=O and C-OH

bond lengths in COOH-functionalised graphene calculated in this study are longer than those calculated for benzoic acid by Chen et al.[S3] whilst the O-H distance in benzoic acid is comparable to that in COOH-functionalised graphene. The carbon atom C9 is as in OH-functionalised graphene, asymmetrically displaced to a position above the plane of graphene resulting in a slight elongation of bond C8-C9 and slight contraction of bond C9-C10 relative to the same bonds on OH-functionalised graphene. The C-H bond makes an angle of 25.2° with the plane through graphene, resulting in a close to parallel orientation of the C-H bond relative to the graphene plane. The optimised position for carbon atom C5 is again an inverted image of the position for C9.

Table S1. Calculated C-C bond lengths[1] in functionalised graphene (bond distance in pristine graphene 1.42 Å)

Bond	Mono-vacancy	OH functionalised	COOH functionalised
$d_{C_1-C_2}$, Å	1.38	**1.43**	**1.44**
$d_{C_2-C_3}$, Å	1.42	1.43	1.43
$d_{C_3-C_4}$, Å	1.42	1.45	1.44
$d_{C_4-C_5}$, Å	1.38	*1.38*	*1.39*
$d_{C_5-C_6}$, Å	1.38	*1.41*	*1.41*
$d_{C_6-C_7}$, Å	1.42	1.45	1.44
$d_{C_7-C_8}$, Å	1.42	1.44	1.44
$d_{C_8-C_9}$, Å	1.38	*1.38*	*1.39*
$d_{C_9-C_{10}}$, Å	1.38	*1.40*	*1.39*
$d_{C_{10}-C_{11}}$, Å	1.42	1.46	1.46
$d_{C_{11}-C_{12}}$, Å	1.42	1.45	1.46
$d_{C_{12}-C_1}$, Å	1.38	**1.42**	**1.44**

[1] Bold: bond adjacent to functional group; Italics: bond adjacent to C-H

2. Description of the adsorption geometries investigated

The square and the hexagonal facet of the Pt_{38}-cluster are indicated in Fig. S2

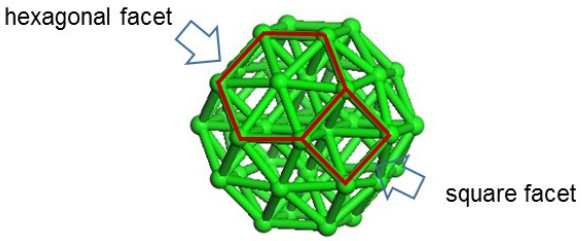

Figure S2: Pt_{38}-cluster with the hexagonal and square facets highlighted

Table S2: Optimised bond lengths for the optimised free unsupported Pt_{38}-cluster

	Square facet	**Hexagonal facet**
d_{Pt-Pt}, Å	2.70, 2.70, 2.70, 2.70	2.70, 2.65, 2.70, 2.65, 2.70, 2.65 (side) 2.70, 2.70, 2.70, 2.70, 2.70, 2.70 (diagonal)

Pt_{38} interaction with pristine and mono-vacancy defective graphene

For adsorption on both pristine and mono-vacancy graphene, two adsorption configurations were investigated. A specific geometry was adsorption via the square facet and the other geometry was through the hexagonal facet. Adsorption was investigated on only one side of the graphene sheet since adsorption through the top and from underneath should be the same owing to the symmetry of the graphene sheet. The initial geometries were such that the atoms on the facet of the cluster approaching the support were placed atop the carbon atoms of the support.

Pt_{38} interaction with OH- and COOH-functionalised graphene

For adsorption on OH- and COOH-functionalised graphene two different adsorption approaches were investigated. The first approach was atop of the graphene on the side bearing the OH-or COOH-functional group. For the atop position the investigated geometry of interaction was limited to the case where the cluster is directly atop the oxygen atom of the OH-or COOH-functional group, with a bond formed between the metal cluster and the OH-or COOH-functional group. Adsorption geometries where the cluster was close by but not interacting with the functional group were not investigated since the aim was to establish the direct role of the functional group on the binding of the cluster.

The second approach was from the underneath side, from this side the cluster is approaching from below the functional group and is not directly attached to the functional group. The adsorption geometries were confined to those where the cluster via its interacting facet were close to the carbon atoms around the vicinity of the added functional group and the saturating H atoms at the vacancy site of the graphene. Only the local region around the added functional group to the graphene was investigated for the binding of the cluster to the support.

On COOH-functionalised graphene a total of 6 adsorption geometries were investigated, with 4 atop geometries and 2 underneath approach geometries. Two variants for both the square and hexagonal facet approach were investigated for the atop geometries. For the square facet approach the first variant is where the square facet approaching the support is at the same level as the COOH group with the O of the C=O group closer to one bridge site of the square facet. The second variant of the square facet approach is the geometry where the square facet approaching the support is not at the same height as the COOH group, but closer to the support with a central Pt atom of the hexagonal facet closest to the O of the C=O group. The two variants for the hexagonal facet approach are identical to those for the square facet approach with the only difference being the hexagonal facet approaching the support instead of the square facet.

On OH-functionalised graphene a total of 4 adsorption geometries were investigated, viz. two atop geometries and 2 underneath approach geometries. The atop geometries consists of the square facet and hexagonal facet approach, with the facet of approach atop the OH- functional group. Similarly for the underneath approach geometries both the interaction via the square and the hexagonal facet were investigated.

3. Optimised adsorption geometries

Adsorption geometries on OH-functionalised graphene

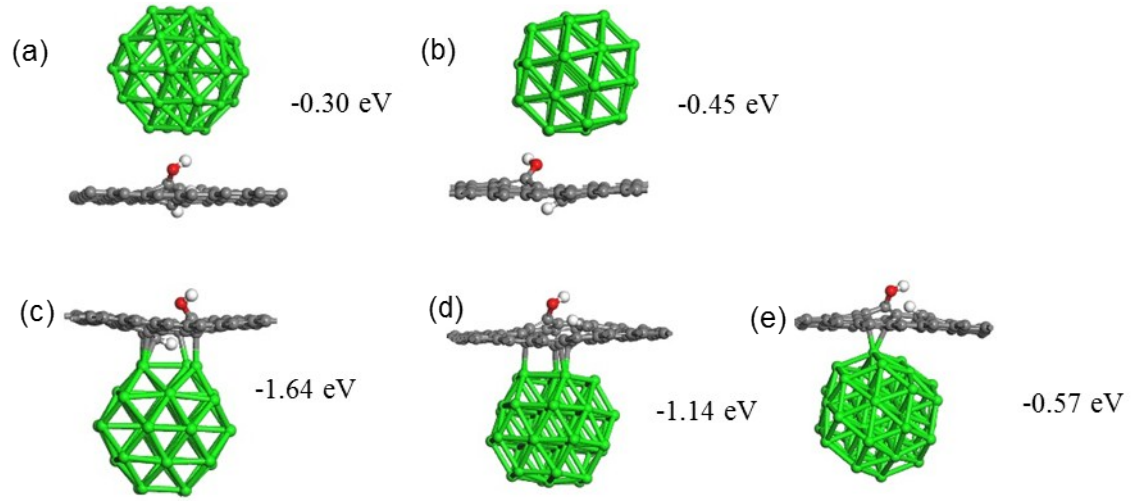

Figure S3: Optimised adsorption geometries of the Pt_{38}-cluster on OH-functionalised graphene together with the PW91 calculated binding energies.

The optimised parameters for the OH functional group in the presence of the adsorbed Pt_{38}-cluster are $d_{C\text{-}O(H)}$ = 1.36Å and $d_{O\text{-}H}$ = 0.98Å, corresponding to a slight bond contraction of 0.02 Å for the C-O(H) bond. Interaction of the Pt_{38}-cluster with OH-functionalised graphene does not significantly change the bond lengths of the OH functional group.

Adsorption geometries on COOH-functionalised graphene

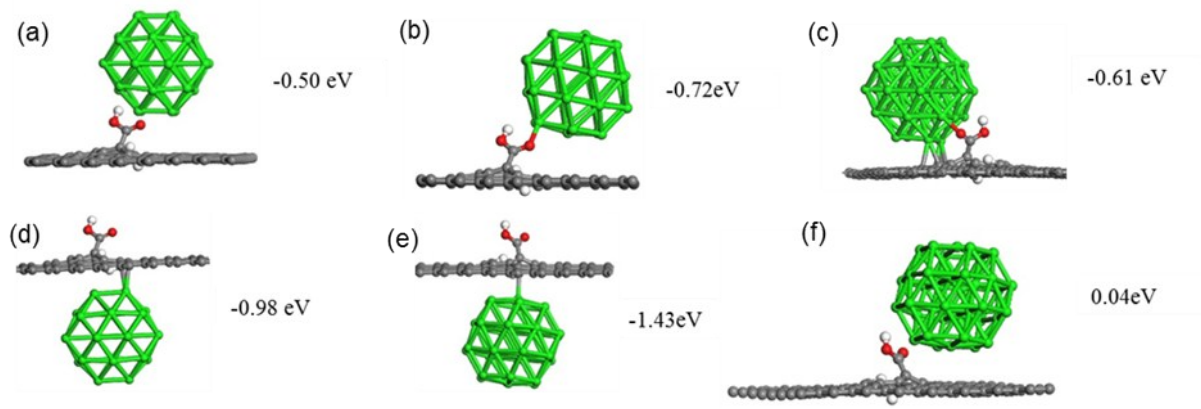

Figure S4*:* Optimised adsorption geometries of the Pt_{38}-cluster on COOH-functionalised graphene together with the PW91 calculated binding energies.

Adsorption of the Pt_{38}-cluster on COOH-functionalised graphene results in distortion of the interacting facet and of the support in the contact region similar to adsorption on the other supports. The optimised parameters for the carboxyl group with the Pt_{38}-cluster approaching via the hexagonal facet are: $d_{C=O}$ = 1.23Å, $d_{C\text{-}O(H)}$ = 1.37Å, $d_{O\text{-}H}$ = 0.98Å and $\angle_{O=C-OH} =$ 120.5°. Hence, the geometry of the COOH functional group does not change much upon adsorption of the Pt_{38}-cluster.

4. Bond lengths of the optimised adsorption geometry using PW91

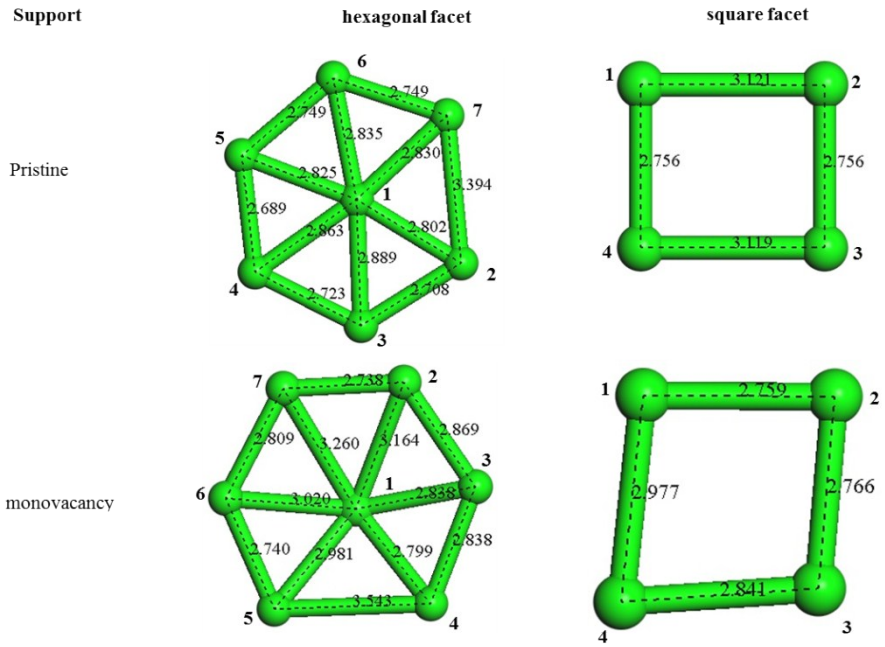

Figure S5: Facet of Pt cluster closest to the support for the Pt_{38}-cluster adsorbed on pristine graphene and mono-vacancy graphene, indicating the Pt-Pt bond distances and the labelling of the Pt atoms.

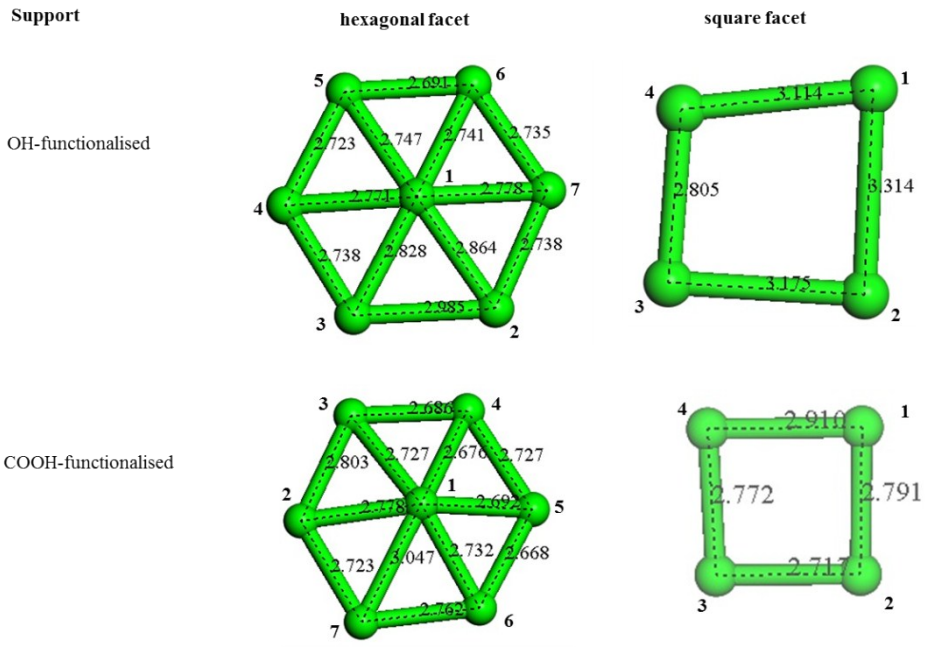

Figure S6: Facet of Pt_{38}-cluster closest to the support for the Pt_{38}-cluster adsorbed on OH-functionalised and COOH-functionalised graphene, indicating the Pt-Pt bond distances and the labelling of the Pt atoms.

5. Comparison of bond length prediction between the PW91 functional and the vdW-OptPBE functional

Table S3: Bond lengths for the optimised Pt_{38}-cluster on pristine graphene calculated with both the PW91 and the vdW-OptPBE functionals

Interaction via	**Square facet**		**Hexagonal facet**			
	PW91	**vdW-OptPBE**	**PW91**		**vdW-OptPBE**	
E_{bind}, eV	0.14	-3.16	3.39		-2.70	
			side	diagonal	side	diagonal
$d_{Pt\text{-}Pt}$ [1], Å	2.76	2.74	3.39	2.83	3.32	2.76
	3.12	3.10	2.75	2.84	2.80	2.75
	2.76	2.75	2.75	2.83	2.79	2.76
	3.12	3.10	2.69	2.86	2.72	2.75
			2.72	2.89	2.72	2.76
			2.71	2.80	2.72	2.76
$d_{Pt\text{-}Pt}$ [2], Å	2.69	2.69	2.64	2.69	2.63	2.69
	2.69	2.69	2.69	2.70	2.70	2.70
	2.69	2.69	2.64	2.71	2.63	2.70
	2.69	2.68	2.71	2.69	2.71	2.69
			2.64	2.71	2.63	2.70
			2.71	2.69	2.71	2.69
$d_{Pt\text{-}C}$, Å	2.20	2.18	2.24		2.29	
	2.19	2.18	2.30		2.32	
	2.19	2.18	2.33		2.32	
	2.20	2.18	2.30		2.29	
			2.44		2.32	
			2.26		2.29	
$d_{C_1\text{-}C_2}$, Å	1.44		1.44			
$d_{C_2\text{-}C_3}$, Å	1.42		1.43			
$d_{C_3\text{-}C_4}$, Å	1.42		1.45			
$d_{C_4\text{-}C_5}$, Å	1.43		1.42			
$d_{C_5\text{-}C_6}$, Å	1.46		1.44			
$d_{C_6\text{-}C_7}$, Å	1.42		1.42			
$d_{C_7\text{-}C_8}$, Å	1.42		1.41			
$d_{C_8\text{-}C_9}$, Å	1.43		1.44			
$d_{C_9\text{-}C_{10}}$, Å	1.44		1.43			
$d_{C_{10}\text{-}C_{11}}$, Å	1.42		1.41			
$d_{C_{11}\text{-}C_{12}}$, Å	1.42		1.41			

[1]Pt-Pt distance of the facet closest to graphene

[2] Pt-Pt distance of the facet opposite and furthest to the one interacting with the graphene

Table S4: Bond lengths for the optimised Pt_{38}-cluster on mono-vacancy graphene calculated with both the PW91 and the vdW-OptPBE functionals

Interaction via	**Square facet**		**Hexagonal facet**			
	PW91	**vdW-OptPBE**	**PW91**		**vdW-OptPBE**	
E_{bind}, eV	-4.31	-5.88	-6.67		-8.46	
			side	diagonal	side	diagonal
$d_{Pt\text{-}Pt}$ [1], Å	2.98	3.04	3.39	2.84	3.74	2.93
	2.84	2.88	2.71	2.83	2.76	2.89
	2.77	2.76	2.72	2.80	2.84	2.81
	2.76	2.75	2.69	2.89	2.75	3.38
			2.75	2.86	2.85	3.03
			2.75	2.83	2.85	3.35
$d_{Pt\text{-}Pt}$ [2], Å	2.75	2.73	2.66	3.16	2.65	2.72
	2.74	2.73	2.69	3.02	2.71	2.71
	2.70	2.71	2.66	3.26	2.66	2.71
	2.72	2.71	2.71	2.84	2.71	2.69
			2.66	2.80	2.68	2.69
			2.70	2.98	2.70	2.70
$d_{Pt\text{-}C}$, Å	1.97	1.97	2.25		2.25	
	2.25	2.25	2.29		2.28	
	2.00	1.99	2.26		2.26	
	1.98	1.98	2.26		2.25	
			2.25		2.23	
			2.26		2.20	
$d_{C_1\text{-}C_2}$, Å	1.45		1.44			
$d_{C_2\text{-}C_3}$, Å	1.45		1.46			
$d_{C_3\text{-}C_4}$, Å	1.43		1.47			
$d_{C_4\text{-}C_5}$, Å	1.44		1.45			
$d_{C_5\text{-}C_6}$, Å	1.44		1.47			
$d_{C_6\text{-}C_7}$, Å	1.45		1.49			
$d_{C_7\text{-}C_8}$, Å	1.49		1.48			
$d_{C_8\text{-}C_9}$, Å	1.46		1.47			
$d_{C_9\text{-}C_{10}}$, Å	1.43		1.44			
$d_{C_{10}\text{-}C_{11}}$, Å	1.44		1.50			
$d_{C_{11}\text{-}C_{12}}$, Å	1.44		1.49			

[1]Pt-Pt distance of the facet closest to graphene

[2] Pt-Pt distance of the facet opposite and furthest to the one interacting with the graphene

Table S5: Bond lengths for the optimised Pt_{38}-cluster on OH- functionalised graphene calculated with both the PW91 and the vdW-OptPBE functionals

Interaction via	**Square facet**		**Hexagonal facet**			
	PW91	**vdW-OptPBE**	**PW91**		**vdW-OptPBE**	
E_{bind}, eV	-1.64	-3.78	-1.14		-3.45	
			side	diagonal	side	diagonal
$d_{Pt\text{-}Pt}$ [1], Å	3.31	3.06	2.69	2.74	2.65	2.71
	3.11	2.76	2.74	2.78	2.70	2.78
	2.81	2.84	2.74	2.86	2.70	2.83
	3.18	2.96	2.99	2.83	2.93	2.82
			2.75	2.77	2.70	2.76
			2.72	2.75	2.70	2.71
$d_{Pt\text{-}Pt}$ [2], Å	2.72	2.70	2.99	2.86	2.69	2.71
	2.73	2.69	2.74	2.83	2.69	2.70
	2.71	2.67	2.72	2.77	2.64	2.69
	2.71	2.67	2.69	2.75	2.63	2.65
			2.74	2.74	2.67	2.65
			2.74	2.79	2.62	2.70
$d_{Pt\text{-}C}$, Å	2.17	2.14	2.17		2.15	
	2.25	2.25	2.27		2.27	
	2.16	2.14	2.26		2.25	
	2.26	2.26				
	2.25	2.21				
	2.24	2.20				
$d_{C_1\text{-}C_2}$, Å	1.45		1.42			
$d_{C_2\text{-}C_3}$, Å	1.49		1.44			
$d_{C_3\text{-}C_4}$, Å	1.46		1.45			
$d_{C_4\text{-}C_5}$, Å	1.43		1.45			
$d_{C_5\text{-}C_6}$, Å	1.44		1.48			
$d_{C_6\text{-}C_7}$, Å	1.45		1.46			
$d_{C_7\text{-}C_8}$, Å	1.44		1.45			
$d_{C_8\text{-}C_9}$, Å	1.44		1.40			
$d_{C_9\text{-}C_{10}}$, Å	1.44		1.40			
$d_{C_{10}\text{-}C_{11}}$, Å	1.44		1.46			
$d_{C_{11}\text{-}C_{12}}$, Å	1.44		1.46			

[1]Pt-Pt distance of the facet closest to graphene

[2] Pt-Pt distance of the facet opposite and furthest to the one interacting with the graphene

Table S6: Bond lengths for the optimised Pt_{38}-cluster on COOH-functionalised graphene calculated with both the PW91 and the vdW-OptPBE functionals

Interaction via	**Square facet**		**Hexagonal facet**			
	PW91	**vdW-OptPBE**	**PW91**		**vdW-OptPBE**	
E_{bind}, eV	-0.98	-3.34	-1.43		-3.52	
			side	diagonal	side	diagonal
$d_{Pt\text{-}Pt}$ [1], Å	2.91	2.87	2.76	2.73	2.81	2.70
	2.77	2.78	2.72	3.05	2.70	3.36
	2.72	2.73	2.80	2.78	2.85	2.79
	2.79	2.78	2.69	2.73	2.68	2.70
			2.73	2.68	2.80	2.66
			2.67	2.69	2.73	2.69
$d_{Pt\text{-}Pt}$ [2], Å	2.72	2.69	2.64	2.71	2.62	2.73
	2.72	2.69	2.69	2.68	2.68	2.66
	2.68	2.65	2.65	2.68	2.63	2.67
	2.72	2.68	2.69	2.71	2.66	2.72
			2.65	2.68	2.64	2.63
			2.69	2.69	2.70	2.69
$d_{Pt\text{-}C}$, Å	2.45	2.36	2.20		2.18	
	2.24	2.24	2.29		2.30	
	2.30	2.25	2.15		2.15	
	2.33	2.30				
$d_{C_1\text{-}C_2}$, Å	1.44		1.43			
$d_{C_2\text{-}C_3}$, Å	1.45		1.45			
$d_{C_3\text{-}C_4}$, Å	1.44		1.43			
$d_{C_4\text{-}C_5}$, Å	1.43		1.43			
$d_{C_5\text{-}C_6}$, Å	1.45		1.46			
$d_{C_6\text{-}C_7}$, Å	1.45		1.46			
$d_{C_7\text{-}C_8}$, Å	1.46		1.46			
$d_{C_8\text{-}C_9}$, Å	1.39		1.43			
$d_{C_9\text{-}C_{10}}$, Å	1.40		1.42			
$d_{C_{10}\text{-}C_{11}}$, Å	1.46		1.44			
$d_{C_{11}\text{-}C_{12}}$, Å	1.45		1.45			

[1]Pt-Pt distance of the facet closest to graphene

[2] Pt-Pt distance of the facet opposite and furthest to the one interacting with the graphene

6. Electronic properties of Pt_{38} interacting with functionalised graphene as determined using the PW91 functional

Polarisation in Pt_{38} cluster upon adsorption

Table S7: Change in the charge on the platinum cluster ($\Delta q_{overall}$), interacting facet ($\Delta q_{interacting\ facet}$), opposite facet to one interacting with the support, i.e. the facet furthest removed from the support ($\Delta q_{opposite\ facet}$) and average change in charge on Pt atoms on half of cluster close to the support[1] ($\bar{q}_{Pt,\,bottom\ half}$) and on Pt atoms in half furthest removed from the support[1] ($\bar{q}_{Pt,\,top\ half}$) based on a Bader charge analysis (negative value indicates charge loss and positive value indicates charge gain).

	Pristine graphene	Mono-vacancy graphene	OH-functionalised graphene	COOH-functionalised graphene
$\Delta q_{overall}$ (e^-)	0.16	-0.44	0.19	0.28
$\Delta q_{interacting\ facet}$ (e^-)	-0.39	-1.14	-0.40	-0.23
$\Delta q_{opposite\ facet}$ (e^-)	0.05	0.03	0.05	0.06
$\bar{q}_{Pt,\,bottom\ half}$[1] ($e^-$/Pt)	0.05	0.04	0.05	0.03
$\bar{q}_{Pt,\,top\ half}$[1] (e^-/Pt)	0.01	0.01	0.01	0.01

1:

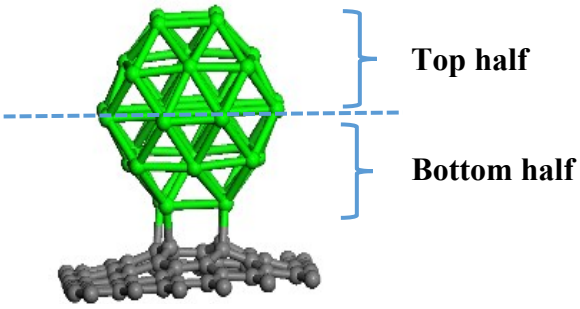

Electron density contour plots

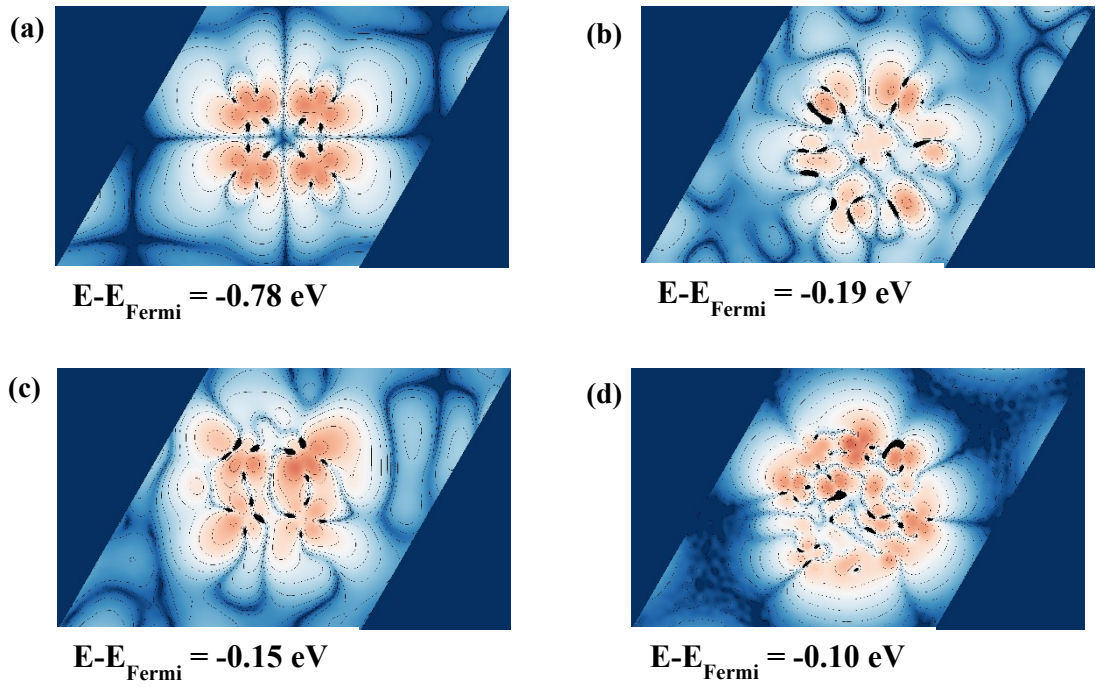

Figure S7: Contour plot of electron density of states in vicinity of Fermi level: (a) Pt_{38} adsorbed on pristine graphene, (b) Pt_{38} adsorbed on mono-vacancy graphene, (c) Pt_{38} adsorbed on OH-functionalised graphene and (d) Pt_{38} adsorbed on COOH functionalised graphene. isosurface level is 0.002 e/Å

Table S8: Binding energies and the d-band centre shift of the Pt_{38}-cluster on the different supports

Support	**$E_{binding}$ (eV)**	**d-band centre shift (eV)**
Pristine graphene	0.14	0.11
Mono-vacancy graphene	-6.67	0.18
OH-functionalised graphene	-1.64	0.33
COOH-functionalised graphene	-1.43	0.23

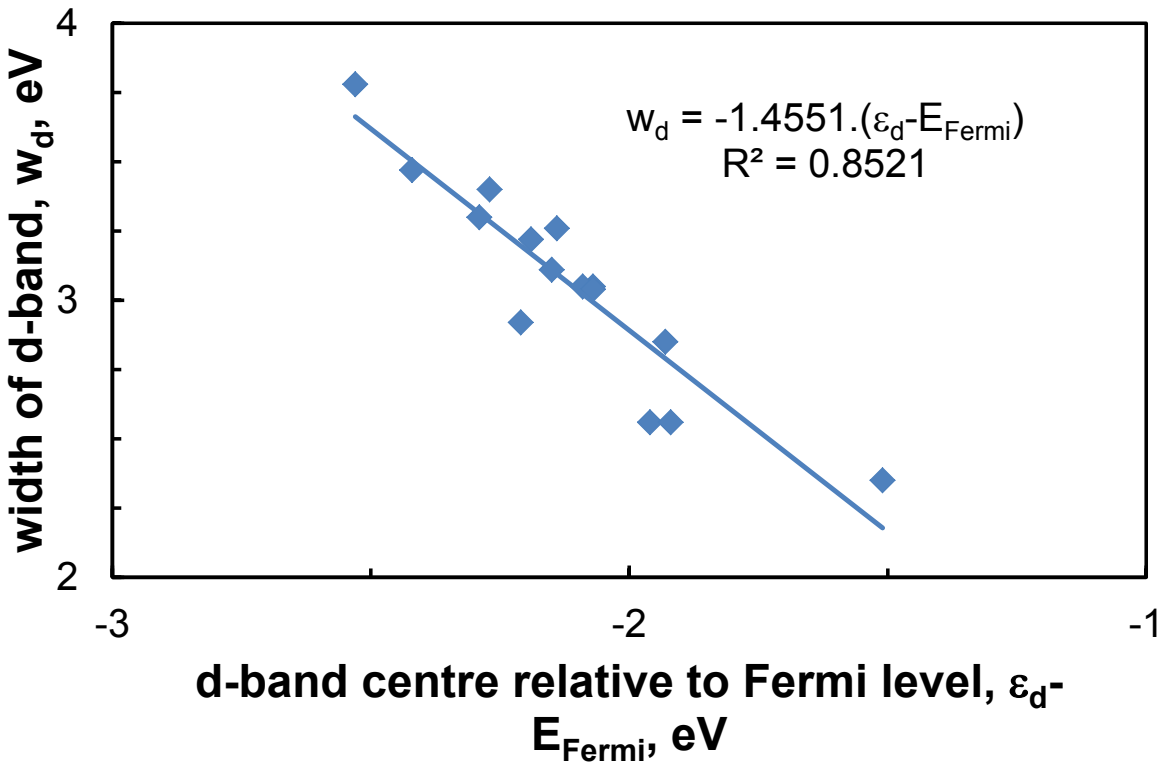

Figure S8: Correlating width of the d-band with the centre of the d-band relative to the Fermi-level for the structures considered

References

[S1] G. Forte, A. Grassi, G,M. Lombardo, A.L. Magna, G.G.N. Angilella, R. Pucci, and R. Vilardi, Phys. Lett. A, 2008, **372**, 6168.

[S2] S.D. Chakarova-Käck, Ø. Borck, E. Schröder and B.L. Ludqvist, Phys. Rev. B, 2006, **74**, 155402.

[S3] W. Chen, C. Tengenkampand and H. Pfnür, Phys. Rev. B, 2009, **79**, 235419.